



25th International Conference on Fracture and Structural Integrity

Mechanical behavior of gas metal arc AA6082-T6 weldments

Francesco Leoni^{*}, Lise Sandness, Øystein Grong, Filippo Berto

Faculty of Engineering, NTNU, Richard Birkelands vei 2B, Trondheim 7491, Norway

Abstract

A series of experiments have been conducted to determine the mechanical properties of AA6082-T6 plates which have been joined by means of the Gas Metal Arc technique. Hardness Vickers tests, bending tests, tensile tests, fatigue tests and Charpy V-notch tests have been carried out to characterize the joints. In addition, an accurate microstructure analysis of selected fracture surfaces has been done. From the tests it is concluded that HAZ softening brings to a reduction in strength with respect to the parent material. It has been noticed that there is a minimum value of hardness in the heat affected zone, that corresponds to the weakest part of the component. From the Charpy V-notch impact tests it has been observed that the material in the HAZ has the highest energy absorption capacity.

© 2019 The Authors. Published by Elsevier B.V.
Peer-review under responsibility of the Gruppo Italiano Frattura (IGF) ExCo.

Keywords: Weldment, GMAW, MIG, Aluminum, Tensile, Fatigue, Charpy, Vickers Hardness.

1. Introduction

One of the most common welding techniques for aluminum alloys is gas-metal arc welding (GMAW), which offers advantages of high-quality welds, high welding speeds and the possibility to be robotized. Even if many improvements have been made in the performance of this process there are many problems associated with fusion welding of the age hardening aluminum alloys. The high coefficient of thermal expansion and solidification shrinkage, combined with a relatively wide solidification-temperature range, makes these alloys susceptible to weld cracking mechanisms like solidification cracking and liquation cracking (Kou (1987)). It is important to characterize the mechanical properties of the joints obtained by welding process to understand the behavior of them when used in structural application. From

^{*} Corresponding author. Tel.: +393473335042.
E-mail address: francesco.leoni@ntnu.no

this reason comes the general purpose of the present report: obtain a better understanding of the mechanical properties of alloy AA6082-T6 subsequent to the gas metal arc welding. To obtain a complete overview of the mechanical properties, hardness, bending, tensile, Charpy V-notch, fatigue tests have been carried out.

Material and methods

1.1. Parent material

In the experimental process of this work, 4 mm extruded plates of aluminum alloy 6082, received in the T6 tempered condition, have been used. The chemical composition of the parent metal is shown in Table 1.

Table 1. Chemical composition of the Parent Metal AA6082.

Si (%)	Fe (%)	Cu (%)	Mn (%)	Mg (%)	Cr (%)	Zn (%)	Ti (%)	Al (%)
0.97-1.00	0.20-0.21	0.02-0.03	0.47-0.48	0.63-0.64	0.00-0.01	0.00-0.01	0.02	Balance

1.2. Filler material

The filler material used in the GMAW process was a 1.2 mm diameter wire of the AA5183 type, with chemical composition as shown in Table 2.

Table 2. Chemical composition of the AA5183 used as filler material.

Si (%)	Fe (%)	Cu (%)	Mn (%)	Mg (%)	Cr (%)	Zn (%)	Ti (%)	Zr (%)	Other (%)
0.40	0.40	0.10	1.00-0.50	5.20-4.30	0.25-0.05	0.25	0.15	-	0.15

Using this filler material gives the following properties (Hobart):

- Excellent strength;
- Excellent ductility;
- Excellent color match;
- Good cracking resistance;
- Good toughness;
- Good corrosion resistance.

1.3. Joining conditions

The weld deposition has been carried out at LEIRVIK with AA5183 as filler wire. The joining conditions are illustrated in the following Figure 1.

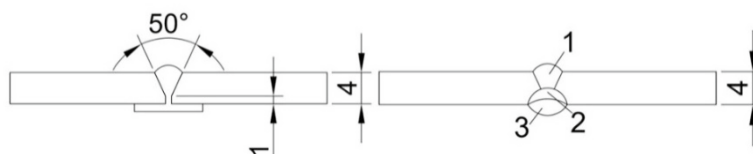


Figure 1. Joining conditions.

Welding parameters can be found in the following Table 3.

Table 3. Welding parameters used in GMAW of AA6082. Two welded plates have been used.

Plate	Elec. Dim	Amps Min-max	Volt Min-max	Heat input (KJ/mm)	Gas Flow Shield (l/min)
1	1.2	180	22	0.43	20
2	1.2	165	22.2	0.3	20

Results and discussion

1.4. Microhardness test

The Vickers hardness (HV) has been measured on one sample. To ensure that the complete HAZ degradation could be revealed, a total length of 150 mm has been kept. A total of three different test series have been conducted. In-between each test series, the sample has been polished. After cutting, the sample has been cold mounted in a ClaroCit acryl resin. The mounted sample has then been ground using SiC grinding paper of increasing fineness (P80, P120, P220, P500, P1000, P2000 and P4000). Water has been used as lubricant. In between each grinding step, the sample has been rinsed in water and then ethanol. The grinding process has been followed by the polishing one, using 3 μm and 1 μm polishing disks and diamond paste suspensions. DP-Lubricant Blue was used as lubricant. After polishing, the samples have been cleaned using an ultrasonic ethanol bath. The parent metal hardness has been measured from ten individual measurements being randomly taken on a specimen of the unaffected parent material. The hardness measurements have been made using a Mitutoyo Micro Vickers Hardness Testing Machine (HM-200 Series) using a load of 1 kg. Following the recommendation in the standard, the distance between each indentation was 0.5 mm, and the full test force was applied for 10 seconds. All these hardness measurements are in accordance with the ASTM E92-17 standard (ASTM (2017)). The Vickers hardness number, in terms of indentation test forces in Newton (N) and indentation diagonals (d_v) measured in millimetres (mm), is calculated as follows:

$$HV = 0.1891 \cdot \frac{F}{d_v^2} \tag{1}$$

In our case, this formula was already implemented in the testing machine.

In Figure 2 it is possible to notice the M-shape, typical of this type of junctions. The reduction of the HV value, confirms the presence of a super-aging (coalescence of β' or β phases) of the alloy that has reduced its mechanical performance (Missori and Sili (2000)). Considering the hardness profile, the minimum HAZ hardness value can be found around 12 mm from the center of the weld on both sides. The minimum HAZ hardness measured are 61 and 58 HV, respectively. A small drop in hardness can be observed at the fusion line. Full recovery of the parent metal hardness is reached approximately 22 mm from the center of the weld.

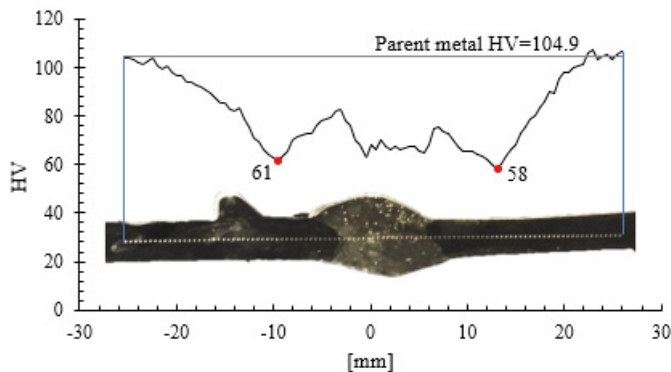


Figure 2: Hardness profile for the GMA weldment, including a macro image of the hardness specimen. The horizontal line at 104.9 represents the HV average value measured on the Parent Metal. The parent metal HV has a standard deviation of 1.7.

1.5. Tensile tests

Tensile test has been carried out following the ASTM E8/E8M – 16a standards (ASTM (2016)). The specimens have been cut from different locations, transverse or longitudinal to the welding direction, to generate specific data for the different weld regions. For the welded ones, two different types of specimens have been tested: one type maintaining the reinforcement, one type machining it. The Fused Zone specimens have been prepared placing the fused part in the center of the specimen. For the HAZ specimens, the center has been chosen using the data of the hardness test, placing the weakest part of the specimens in the center. The tests have been done by using a MTS servo-hydraulic tensile machine. The axial elongation has been measured using an extensometer with 25 mm gauge length. The cross-head speed has been fixed to $v = 1.5 \text{ mm/min}$, which corresponded to a strain rate of $\dot{\epsilon}_{nom} = 10^{-3} \text{ s}^{-1}$. The results are summarized in Table 4.

The behaviour of the welded specimens appears similar in both the machined or in the ones where the reinforcement has been taken. The small difference between those can be due to the different thickness: the machined ones have a very small thickness which can affect the behaviour during the test, taking the material to a condition of plane stress. To have a quick comparison between the results of the tests the following summary Table 4 is presented. The reduction in area of the specimens tested has been calculated using the following Equation 2:

$$red\% = \frac{A_f - A_i}{A_i} \cdot 100 \quad (2)$$

Where A_f is the cross-section area after testing, A_i is the cross-section area of the specimen before testing.

Table 4: Tensile test results summary table. The values are the average of three measurements.

	E (GPa)	$\sigma_{p,0.2}$ (MPa)	UTS (MPa)	Reduction in area (%)
Parent material transverse	70.7	317	336	18
Parent material longitudinal	65.9	314	335	22
Fused zone longitudinal	65.7	132	216	15
HAZ longitudinal	62.8	145	210	53
Fused zone machined	64.0	115	176	68
HAZ machined	62.9	118	175	71
Fused zone	67.0	142	213	56
HAZ	54.4	141	211	59

The strength in the welded specimens is around half the one from the parent metal. All the tensile specimens broke in the Heat Affected Zone approximately 10 mm from the welding center. This corresponds well with observations made from the hardness profile, where the minimum hardness is found in HAZ on the side without the guide for the welding tool (the plate had that guide because the same Parent Metal plates were used for the HYB process). Considering the correlation between hardness and yield strength, the resulting yield strength profile for the welded plates can be calculated based on the following Equation 3 and the experimental hardness profiles (Grong (1997)).

$$\sigma_y = 3 \cdot HV - 48 \quad (3)$$

1.6. Fatigue tests

Fatigue test has been carried out following the ASTM E466 – 15 standards (ASTM (2015)). The practice used gives the indications for the performance of axial force-controlled fatigue tests to obtain the fatigue strength of metallic materials in the fatigue regime where the strains are predominately elastic (ASTM (2015)).

The specimens have been taken from the parent metal both longitudinal and transverse to the extrusion direction. The welded specimens have been taken in two different ways: one centering the welding, one centering the weakest part of the plate (basing on the tensile and hardness tests results). For all the fatigue specimens, the reinforcements have been taken. The ratio chosen for the tests is R= 0.1. To obtain a S-N curve, the stresses to be applied have been calculated by considering the tensile test results. The stress amplitude range used goes from 112 MPa to a minimum of 40 MPa. Considering the stress chosen, knowing the measures of each specimen, the forces have been set on the fatigue machine. The fatigue tests have been performed by using a standard MTS servo hydraulic machine. The frequency chosen for the tests was 10 Hz.

The difference between the FZ and HAZ fatigue specimens consists in the position of the geometrical center of the tested zone. In the FZ specimens the fused zone has been taken in the center, in the case of HAZ, the center corresponds with the weakest part of the specimens in accordance to the hardness profile measured. This differentiation appears to not have effect on the breaking mechanism: as expected all the fatigue specimens failed starting from the welding toe, where the stress concentration occurs. In simple components as in our case, the nominal stress can be determined using the following Equation 4.

$$\sigma = \frac{F}{w \cdot t} \tag{4}$$

F is the force set in the testing machine, w is the width of the specimen and t the thickness.

Many of the welded specimens tested were misaligned. Following the indication in the standard, the effect of misalignment can be considered applying an additional stress raising factor k_m (Hobbacher (2009)). A formulation of the stress raising factor k_m is provided as follows:

$$k_m = 1 + \frac{3 \cdot \alpha \cdot l \cdot \tanh\left(\frac{\beta}{2}\right)}{2 \cdot t \cdot \left(\frac{\beta}{2}\right)} \tag{5}$$

Where α is the angle of misalignment, l is the half length of the specimen tested, t the specimen thickness, and β can be estimated accordingly to the following expression:

$$\beta = \frac{2 \cdot l}{t} \cdot \sqrt{\frac{3 \cdot \sigma}{E}} \tag{6}$$

Where E is the Young’s modulus. To provide a more complete overview of the behavior of the material, the results are presented both using the correction and in the original values. The standard is referred to a PS-95%. Table 5 provides the overview of the fatigue test results, giving the values of the k as an indication of the Basquin slope of the S-N (log-log) resulting graphs.

Table 5: Fatigue tests summary table.

	Parent material transverse	Parent material longitudinal	Welded material No K_m	Welded material considering K_m	Standard for welding
k	3,9	3,7	3,8	2,8	3
$\Delta\sigma_{(95\%)(2e6)}$	62	64	31	27	25

The typical value of k is 4 for the parent material, and this value is in accordance to what has been found from the tests. For the welding, the standard provides a value of k equal to 3. As can be seen in Table 5, the experimental results are in accordance to that indication. Another parameter to compare is the value of stress at 2×10^6 cycles, which is 25 in the standard under consideration. The results show that this value is closer to the standard when misalignment effect is considered applying the K_m factor. As a conclusion, it can be said that the standard gives good indications for the case considered herein.

1.7. Bending test

Bending tests have been carried out following the NS-EN ISO 5173:2009 standards (NS-EN ISO (2009)). In the three-point bend tests the specimens are bent into the die by a plunger (Figure 3). The convex surface of the bent specimen is then examined for cracks or other defects. This test is used to evaluate the quality of the welds as a function of the ductility as evidenced by their ability to resist cracking during large deformation. Rectangular specimens from plates have been tested. The measures of the specimens and the radius of the rollers are shown in the following Figure 3.

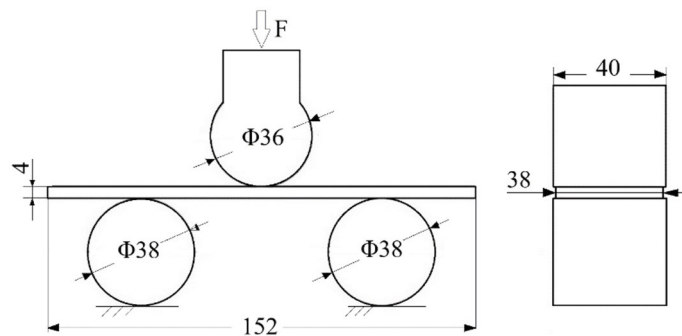


Figure 3: Bend test set-up.

Some grease has been used between the rollers and the specimen. After bending, the convex surface of the bent specimen has been examined to check the presence of any cracks or other defects. The tests have been stopped in case of cracks propagated through the whole thickness or at the end of the plunger stroke. The tests have been done using a MTS 809 Axial Test System, setting the speed of the plunger to 1 mm/min. The welded specimens appear to be more ductile, since no cracks were visible. This result is also confirmed by the tensile and Charpy tests. In the following graphs, the force applied with the plunger is plotted as function of the stroke of it.

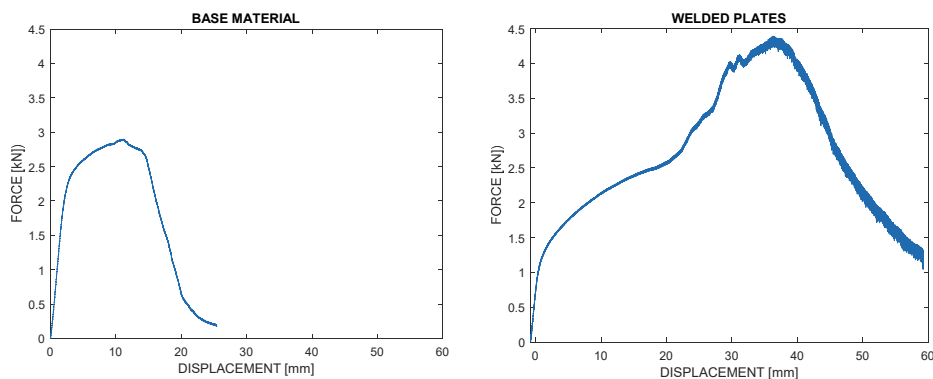


Figure 4: Force applied with the plunger on the Parent material (on the left) and on the welding (on the right).

As can be seen in the plots, the force in the parent material test goes down to zero. This because the crack propagates

through the whole thickness of the specimens. The second plot is referred to the welded specimen. The force does not go down to zero, and the test has been stopped not because the specimen failed but because the plunger reached the maximum stroke.

1.8. Charpy test

Impact data have been collected by performing some Charpy V-notch tests. The tests have been carried out following the ASTM E23 – 16b standard (ASTM International (2016)). Charpy test has been used to get information about the energy absorbed during the impact. Specimens from the parent metal, fusion zone and HAZ in the same direction and orientation as the tensile test specimens have been tested. The testing machine used for the tests was a Zwick/Roell RKP450. The basic dimensions of the Charpy test specimens are shown in the following Figure 5. The 2.5 mm thickness has been chosen because the welded plates were distorted, and in the transverse case, maintaining the original thickness of the plates brought to a not straight specimen.

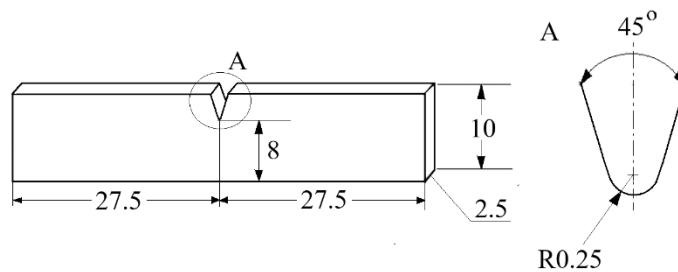


Figure 5: Geometry of the Charpy specimens tested.

In the following Table 6, the average values of the absorbed energy are presented.

Table 6: Summary table of the Charpy test results. The material in the heat affected zone has the greatest energy absorption capacity

	Parent Metal Transverse	Parent Metal Longitudinal	Fused zone Longitudinal	HAZ Longitudinal	Fused zone Transverse	HAZ Transverse
Energy (J)	4.2	4.9	3.0	8.2	3.9	8.4

Conclusions

From the analysis of the results obtained it can be concluded the following:

- The hardness profile is as expected, the typical “M” shape is due to the microstructure modifications that occurs because of the heat input during the fusion welding. The lowest value of hardness found in the HAZ brings to a reduction in strength that has to be taken into account in the structural design. This reduction in strength has been proved also with the tensile test: all the welded specimens broke in the HAZ, where the point of minimum hardness was measured.
- The bend test reveals the good quality of the GMAW studied: the specimens didn’t show the formation of cracks during the bend test, and the amount of welding defects is very low.
- From the fatigue test it has been observed that the model provided for the study of misaligned specimens is useful and it is in accordance with the results obtained. In particular it has been seen that using the correction factor indicated in the standard makes the fatigue results matching to the standard indications.
- The Charpy impact test confirmed what found with the tensile test, showing how the more ductile behavior of the softened HAZ brings to a higher energy absorption capacity.

- The aluminum alloy tested as parent material has a high mechanical strength. The results are overall in accordance to what indicated in literature for this kind of aluminum alloy.

References

- ASTM, 2015, Standard Practice for Conducting Force Controlled Constant Amplitude Axial Fatigue Tests of Metallic Materials 1.
- ASTM, 2016, Designation: E8/E8M – 16a Standard Test Methods for Tension Testing of Metallic Materials 1.
- ASTM, 2017, *Standard Test Methods for Vickers Hardness and Knoop Hardness of Metallic Materials*.
- ASTM International, 2016. *E23-16b Standard Test Methods for Notched Bar Impact Testing of Metallic Materials 1*.
- Grong, Ø., 1997, *Metallurgical Modelling of Welding / Øystein Grong. - Version Details - Trove*.
- Hobart, Aluminum Filler Metal Selection Chart, (https://www.hobartbrothers.com/downloads/aluminum_selecti_110o.pdf).
- Hobbacher, A., 2009, *Recommendations for Fatigue Design of Welded Joints and Components*. New York, NY: Welding Research Council.
- Kou, S., 1987. *Welding Metallurgy*. 2nd ed. New Jersey.
- Missori, S., Sili, A., 2000, *Mechanical Behavior of 6082-T6 Aluminum Alloy Welds*.
- NS-EN ISO, 2009, Amendment A1 - Destructive Tests on Welds in Metallic Materials - Bend Tests - Amendment 1 (ISO 5173:2009/Amd 1:2011).